ISBN: 978-3-95450-214-1 ISSN: 2673-5490 doi:10.18429/JACoW-IPAC2021-MOPAB301

A CONCEPT FOR RECONSTRUCTION OF THE CAPSULATED MICROCHIP STRUCTURE USING ITS INTERACTION WITH HIGH-ENERGY ION BEAMS OF THE NICA ACCELERATOR COMPLEX*

A. Slivin†, A. Butenko, G. Filatov, E. Syresin, A. Tuzikov, A. Zhemchugov
Joint Institute for Nuclear Research, Dubna, Russia

Abstract

Within the framework of the NICA project an applied research station for irradiation by long-range ions (SODIT) is being constructed for testing radiation hardness of semiconductor micro- and nanoelectronics products in the energy range of 150-350 MeV/n. Calculations for the interaction of high-energy gold ions with the microchip and strip detector structures are performed using the GEANT4 simulation toolkit. A concept was developed for reconstruction of the capsulated microchip structure in terms of depth and in terms of cross-section using interaction with high-energy ions at the technical station for irradiation by long-range ions. The possibility of localizing the radiation-vulnerable area of the microchip is evaluated.

INTRODUCTION

Modern radio-electronic systems used on board spacecraft have to operate under hard conditions, being exposed to cosmic particles. In order to research and test promising semiconductor micro- and nanoelectronics products for resistance to heavy charged space particles and single radiation effects, a technical station for irradiation by long-range ions (SODIT) is under construction in the Measurement Hall of Building 1 of the Veksler and Baldin Laboratory of High Energy Physics (VBLHEP) [1, 2].

The SODIT station includes a specialized detector part (DPS-NICA), which was designed for precision localization of the particle track and energy release in a microchip and localization of vulnerable areas of microchips (determination of the sample profile and localization of the microchip crystal) [3, 4]. The detector part consists of a set of silicon pad and strip planes located in front of and behind the sample. The structure of the detector is described in detail below.

SIMULATION OF HIGH-ENERGY ION INTERACTION WITH MATERIALS OF CAPSULATED MICROCHIPS

Simulation of high-energy $^{197}Au^{79}$ beam interactions with semiconductor microelectronics using the GEANT4 [5] software package is presented.

Here the ion beam successively passes through the following geometry elements: a round titanium foil 0.05 mm thick (radius 140 mm) at the ion beam output, an air layer 500 mm thick, a pad silicon plane 0.3 mm thick (square cross-section 40x40 mm) of the detector, an air layer 20 mm thick, two pairs of strip (track) silicon planes 0.3 mm thick (square cross-section 40x40 mm) with an air gap 20 mm thick between them. Behind the second pair of detectors, there is another 20-mm-thick air gap.

Then a sample microchip was simulated, which included a nickel cover 0.3 mm thick (square cross-section 40x40 mm), a silicon chip 0.5 mm thick (square cross-section 20x20 mm) inside the ceramic cavity (thickness of the thick layer at the edges of the microchip is 1.5 mm, thickness of the thin layer behind the microchip is 1 mm, square cross-section is 40x40 mm), and a fiberglass layer 2 mm thick (square cross-section 60x60 mm).

Behind the 15-mm-thick air layer, downstream of the sample microchip, there is a detector system that includes two pairs of silicon strip (track) planes 0.3 mm thick (square cross-section 40x40 mm) with an air gap of 10 mm between them.

Considering the air interlayers, the total thickness of the entire geometry along the beam path is 591.5 mm.

The general view of the geometry is shown in Fig. 1.

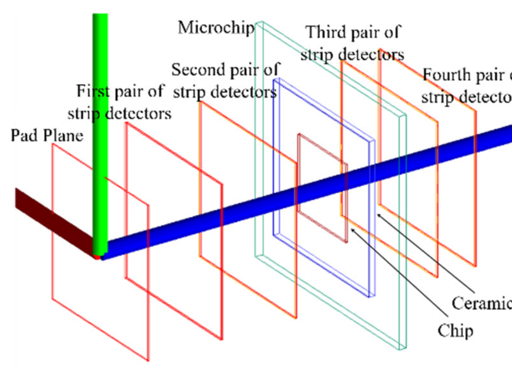

Figure 1: The geometry's target unit (sample microchip, set of detectors in front of and behind sample microchip).

The passage of the ion beam through the geometry changes the ion beam energy, as well as the ionization capacity of the beam, so that it is possible to study the internal structure of the microchip as a function of energy distribution and to perform so-called microchip tomography by measuring the energy of ions at the output of the microchip with two orthogonal strip detectors [3, 4].

Localization of the Radiation-Vulnerable Areas of the Microchip

An option was considered where the microchip with the package is irradiated by an ion beam with a diameter of 400 μm at half maximum, namely, a beam of $^{197}Au^{79}$ ions with the initial energy of 300 MeV/n and charge of 79.

*Work supported by grant for young scientists. Unique ID 21-102-09
†slivin@jinr.ru

ISBN: 978-3-95450-214-1 ISSN: 2673-5490 doi:10.18429/JACoW-IPAC2021-MOPAB301

Moving along the longitudinal axis, this ion beam successively passes through the titanium foil, the detector pad plane, two pairs of strip (track) planes, and the nickel cover of the microchip and arrives at the interface between the silicon microchip and the ceramics so that half of the beam hits the ceramics and the other half hits the silicon microchip. The output data were read out from the silicon strip detector 300 μm thick (square cross-section 40x40 mm, strip width 25 μm was selected to be 4 times smaller than in the real DPS-NICA detector [3, 4]) following the fiberglass layer. The characteristic size of the radiation-vulnerable element is on the order of 10x10 μm, thus, the task with obtaining a spatial resolution less than 10 μm is most interesting. To solve the problems associated with the localization of the microchip crystal, it is necessary to implement the attachment of the crystal to the DPS-NICA detector with maximum accuracy. For this purpose, the possibility of reducing the width of the strip planes from 100 μm to 25 μm was considered.

The distribution of energy peaks over the coordinates of the strips' midpoints near the silicon–ceramic interface (coordinate 10 mm) is shown in Fig. 2.

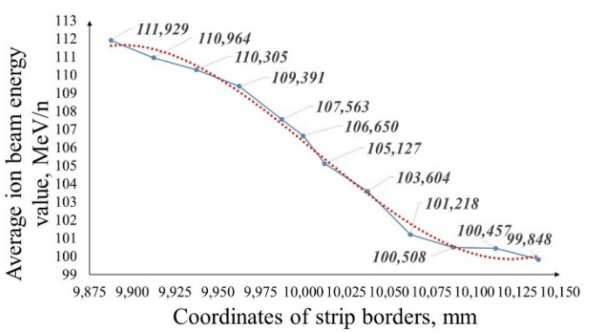

Figure 2: Distribution of energy peaks over strips.

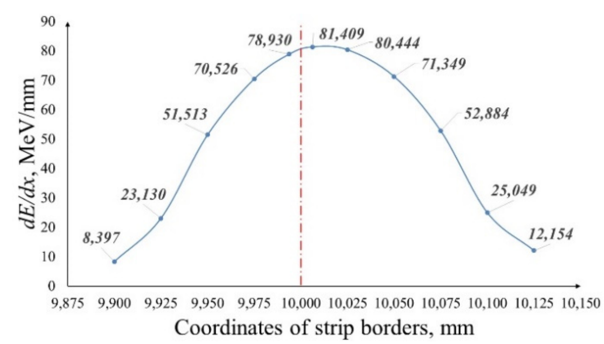

Figure 3: The derivative of the energy peaks in the transverse plane (over strips).

The distribution of the energy peak derivatives in Fig. 3 is shifted to the right relative to the silicon-ceramic (coordinate 10 mm). The maximum derivative value is 81.409 MeV/mm and is shifted by 5 μm to the right. Thus, without knowing the position of the silicon active part of the microchip relative to the detector, with a selected strip width of 25 μm, it is possible to determine the interface between the two materials with an accuracy of 5 μm and reconstruct its position with this accuracy. The full width at half maximum of the peak derivative of ionization losses (Fig. 3) is about 100 μm and is determined by the effects of angle scattering of ions in the microchip materials.

A Concept for Reconstruction of the Capsulated Microchip Structure in Terms of Depth

An iterative method is used to determine the depth structure of the microchip. The principle of the method is to determine the thicknesses of the microchip nickel cover and the ceramics when the total thickness of the microchip is known. The layer thicknesses were determined by the iterative method based on analytical calculations of ionization losses and Geant4 calculations using the known energy of ions at the entrance and exit of the microchip. The total thickness of the microchip is measured with a micrometer and initially assumed to be known. It is 1800 μm in the calculations below.

For the $^{197}Au^{79}$ ion beam with the initial energy of 300 MeV/n and charge of 79, the dependence of the nickel cover thickness on the total thickness of the microchip (green straight line in Fig. 4) is constructed on the basis of the Bethe-Bloch formula for particle ionization losses.

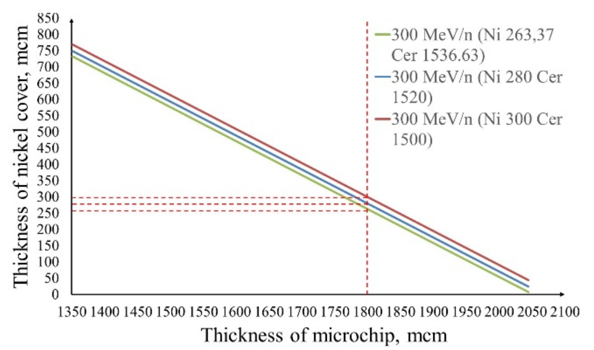

Figure 4: The dependence of the thickness of the nickel cover on the thickness of the microchip.

According to Fig. 4, the thickness of the nickel cover is 263.374 μm while the total thickness of the microchip is 1800 μm. The thickness of the ceramic layer in the microchip will then be 1536.626 μm. Simulations were performed using the GEANT4-obtained layer thicknesses. The average energy of the ion beam at the microchip output is 173.25 MeV/n, which is 0.98% higher than the incoming value.

In order to achieve equality between the average output energy of the ion beam and the incoming beam energy, it is necessary to increase the thickness of the nickel cover while reducing the thickness of the ceramic layer because the nickel cover (density 8.907 g/cm^3) is denser than the ceramic material (Al_2O_3 with a density of 3.97 g/cm^3).

The thickness of the nickel cover was increased to 280 μm while the microchip thickness remained to be 1800 μm, and the thickness of the ceramic thus reduced to 1520 μm. An average ion beam output energy is 172.48 MeV/n, which is 0.53% higher than the incoming value. The corresponding plot is the blue straight line in Fig. 4.

The thickness of the nickel cover was increased to 300 μm, and the thickness of the ceramic was reduced to

ISBN: 978-3-95450-214-1 ISSN: 2673-5490 doi:10.18429/JACoW-IPAC2021-MOPAB301

1500 µm. With a nickel cover thickness of 300 µm and a ceramic thickness of 1500 µm, the average energy of the ion beam at the microchip output is 171.62 MeV/n, which is 0.03% higher than the incoming value. The corresponding plot is the red straight line in Fig. 4.

The iterative method described above is able to determine the set thicknesses of the nickel cover and the ceramic of the microchip.

The microchip is fixed on a fiberglass layer in the calculation model. The thickness of the fiberglass layer can be accurately measured, and it is 2000 µm in the described model. Using the iterative method described above and knowing the layer thickness and the average output energy of the ion beam from the fiberglass layer, one can determine the average energy of the ion beam at the entrance to the layer (it is also the average output energy from the ceramic layer, incoming beam energy).

The Thickness of the Silicon Chip inside the Ceramic Cavity

The calculation of the thickness of the silicon chip inside the ceramic cavity is presented below. Figure 5 shows the output energy spectrum of the ion beam at the exit from the ceramic layer when the ion beam passes through the centre of the chip (distance 5 mm in transverse plane) successively moving through the nickel cover, the silicon chip and the ceramic layer thick 1000 µm.

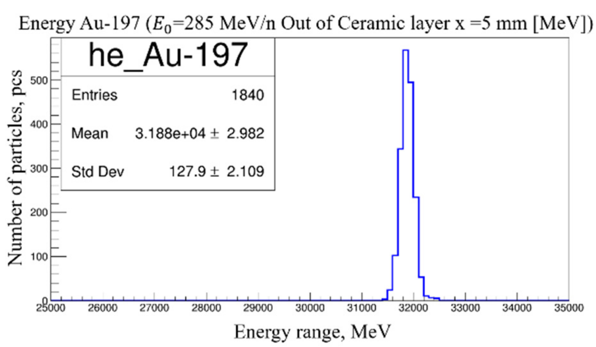

Figure 5: Energy spectrum of the ion beam at the exit from the ceramic layer after passing through distance 5 mm (an average energy of the ion beam is E_1=161.83 MeV/n).

Figure 6 shows the output energy spectrum of the ion beam at the exit from the ceramic layer when the ion beam passes through the edge of the chip (distance 15 mm in the transverse plane) successively moving through the nickel cover and the ceramic layer thick 1500 µm.

Solving the system of equations constructed on the basis of the Bethe-Bloch formula for particle ionization losses for two cases where ions pass through the silicon chip and where they do not, we find that the calculated thickness of the silicon chip is 494.2 µm. With the actual silicon chip thickness of 500 µm given in the GEANT4 model, the calculation error is 1.17%.

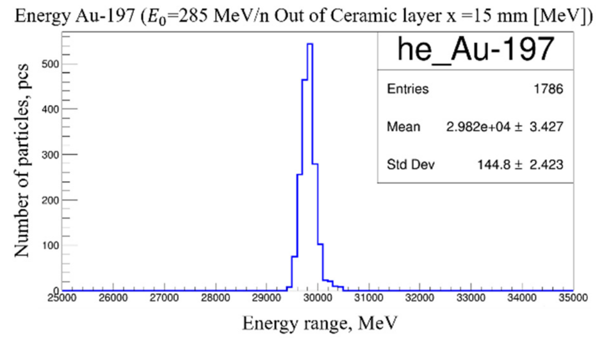

Figure 6: The energy spectrum of the ion beam at the exit from the ceramic layer after passing through distance 15 mm (an average energy of the ion beam is E_2=151.37 MeV/n).

CONCLUSION

Calculations for the interaction of high-energy gold ions with the microchip and strip detector structures were performed using the GEANT4 simulation toolkit. Transverse tomography of the microchip structure in terms of the energy distribution of ions was proposed in [3]. Through a transition from 100-µm-wide strip to the 25-µm-wide strip, the calculations showed that the accuracy of determining the position of the active silicon chip inside the microchip was 5 µm. A concept was proposed for reconstruction of the capsulated microchip structure in terms of depth and in terms of cross-section using interaction with high-energy ions at the technical station for irradiation by long-range ions.

Experimental verification of the microchip structure reconstruction based on tomography of the ion energy distribution by a strip detector is planned for 2022.

ACKNOWLEDGEMENTS

Work supported by grant for young scientists. Unique ID 21-102-09.

REFERENCES

[1] E. Syresin *et al.*, "New Nuclotron beam lines and stations for applied researches", in *Proc. 10th Int. Particle Accelerator Conf. (IPAC'19)*, Melbourne, Australia, May 2019, pp. 449-451. doi:10.18429/JACoW-IPAC2019-MOPMP013

[2] A. Slivin *et al.*, "Development of beam diagnostics systems for applied experimental stations at VBLHEP JINR", in *Proc. AIP*, Oct. 2019, vol. 2163, pp. 080007. doi: 10.1063/1.5130122

[3] O. Vasilev *et al.*, "Preliminary Simulation Results for the DPS-NICA Project", *Phys. Part. Nuclei Lett.*, vol. 17, pp. 871–877, 2020. doi:10.1134/S1547477120060138

[4] O. Vasiliev *et al.*, "Detector Part of the Station for the Research and Irradiation of Promising Products of Semiconductor Micro- and Nanoelectronics with High-Energy Ion Beams", *Phys. Part. Nuclei Lett.*, vol. 18, pp. 213–219, 2021. doi: 10.1134/S1547477121020205

[5] S. Agostinelli *et al.,* "Geant4—a simulation toolkit", *Nucl. Instrum. Methods Phys. Res. A.*, vol 506, pp. 250–303, 2003. doi:10.1016/S0168-9002(03)01368-8